Immune Netw. 2021 Aug;21(4):e31
https://doi.org/10.4110/in.2021.21.e31
pISSN 1598-2629·eISSN 2092-6685

IMMUNE NETWORK

Original Article

Tumor-Infiltrating Neutrophils and Non-Classical Monocytes May Be Potential Therapeutic Targets for HER2^{negative} Gastric Cancer

Juhee Jeong [1,2], **Duk Ki Kim**[1,2], **Ji-Hyeon Park** [3], **Do Joong Park** [3,4,5], **Hyuk-Joon Lee** [3,4,5], **Han-Kwang Yang**[3,4,5], **Seong-Ho Kong**[3,4,5,*], **Keehoon Jung** [1,2,6,*]

[1]Department of Anatomy and Cell Biology, Seoul National University College of Medicine, Seoul 03080, Korea
[2]Department of Biomedical Sciences, Seoul National University College of Medicine, Seoul 03080, Korea
[3]Department of Surgery, Seoul National University Hospital, Seoul 03080, Korea
[4]Department of Surgery, Seoul National University College of Medicine, Seoul 03080, Korea
[5]Cancer Research Institute, Seoul National University, Seoul 03080, Korea
[6]Institute of Allergy and Clinical Immunology, Seoul National University Medical Research Center, Seoul 03080, Korea

Received: Jul 7, 2021
Revised: Aug 9, 2021
Accepted: Aug 10, 2021

***Correspondence to**
Keehoon Jung
Department of Anatomy and Cell Biology, Seoul National University College of Medicine, 103 Daehak-ro, Jongno-gu, Seoul 03080, Korea.
E-mail: keehoon.jung@snu.ac.kr

Seong-Ho Kong
Department of Surgery, Seoul National University Hospital, 101 Daehak-ro, Jongno-gu, Seoul 03080, Korea.
E-mail: seongho.kong@snu.ac.kr

ORCID iDs
Juhee Jeong
https://orcid.org/0000-0003-4732-147X
Ji-Hyeon Park
https://orcid.org/0000-0002-6811-8895
Do Joong Park
https://orcid.org/0000-0001-9644-6127
Hyuk-Joon Lee
https://orcid.org/0000-0002-9530-647X
Keehoon Jung
https://orcid.org/0000-0002-2199-5292

ABSTRACT

Gastric cancer (GC) is the fourth most common cause of cancer-related death globally. The classification of advanced GC (AGC) according to molecular features has recently led to effective personalized cancer therapy for some patients. Specifically, AGC patients whose tumor cells express high levels of human epidermal growth factor receptor 2 (HER2) can now benefit from trastuzumab, a humanized monoclonal Ab that targets HER2. However, patients with HER2^{negative} AGC receive limited clinical benefit from this treatment. To identify potential immune therapeutic targets in HER2^{negative} AGC, we obtained 40 fresh AGC specimens immediately after surgical resections and subjected the CD45^{+} immune cells in the tumor microenvironment to multi-channel/multi-panel flow cytometry analysis. Here, we report that HER2 negativity associated with reduced overall survival (OS) and greater tumor infiltration with neutrophils and non-classical monocytes. The potential pro-tumoral activities of these cell types were confirmed by the fact that high expression of neutrophil or non-classical monocyte signature genes in the gastrointestinal tumors in The Cancer Genome Atlas, Genotype-Tissue Expression and Gene Expression Omnibus databases associated with worse OS on Kaplan-Meir plots relative to tumors with low expression of these signature genes. Moreover, advanced stage disease in the AGCs of our patients associated with greater tumor frequencies of neutrophils and non-classical monocytes than early stage disease. Thus, our study suggests that these 2 myeloid populations may serve as novel therapeutic targets for HER2^{negative} AGC.

Keywords: Neutrophils; Non-classical monocytes; Tumor microenvironment; Immunotherapy; Gastric cancer

IMMUNE NETWORK

Conflict of Interest
The authors declare no potential conflicts of interest.

Abbreviations
AGC, advanced gastric cancer; CI, confidence interval; FSC-A, forward scatter area; GC, gastric cancer; GEO, Gene Expression Omnibus; HER2, human epidermal growth factor receptor 2; HR, hazard ratio; OS, overall survival; PMN-MDSC, polymorphonuclear myeloid-derived suppressor cell; TCGA, The Cancer Genome Atlas; TME, tumor microenvironment.

Author Contributions
Conceptualization: Kong SH, Jung K; Investigation: Jeong J, Kim DK, Jung K; Supervision: Jung K; Surgery: Park JH, Park DJ, Lee HJ, Yang HK, Kong SH; Writing - original draft: Jeong J, Jung K; Writing - review & editing: Kong SH, Jung K.

INTRODUCTION

Gastric cancer (GC) remains a major contributor to the global cancer burden (1): the Global Cancer Observatory reported that in 2020, there were more than 1 million new GC cases worldwide and over 750 thousand GC-related deaths. As a result, GC ranks fifth and fourth in terms of cancer incidence and mortality, respectively (2). Eastern Asia has the highest incidence of GC for both men and women (2).

Currently, the standard therapeutic regimens for unresectable or metastatic advanced GC (AGC) are chemotherapeutic agents such as platinum compounds, fluoropyrimidines, paclitaxel, docetaxel, and irinotecan (3). However, due to the evolution of drug resistance in the tumor microenvironment (TME), these therapies have limited clinical efficacy in terms of median overall survival (OS) (4), which ranges from 13.0 to 14.1 months (5). The mechanisms underlying this chemoresistance remains poorly understood, largely because the gastric TME contains many different cell types (e.g. endothelial cells, stem cells, T cells, myeloid cells such as monocytes, macrophages, dendritic cells, and neutrophils), all of which interact with each other and the GC cells *via* extremely complicated pathways (6).

Recent advances in the GC field have led to a new classification of AGCs that is based on molecular features and may lead to personalized and potentially more effective therapy (7). One of these subtypes is characterized by overexpression or amplification of human epidermal growth factor receptor 2 (HER2). HER2 is an important mediator of cancer cell proliferation and differentiation and its overexpression in several cancers associates with rapid tumor growth and metastatic activity. Between 7% and 27% of AGCs overexpress this biomarker (8). Recently, the United States Food and Drug Administration approved trastuzumab, a human monoclonal Ab that targets HER2 proteins on cancer cells, for treating metastatic HER2-positive GC, breast cancer, and esophageal cancer (9,10). By binding to HER2, trastuzumab inhibits the HER2-mediated activation of downstream signaling pathways such as the MAPK and PI3K/Akt pathways. The binding event both suppresses cancer cell growth and triggers Ab-dependent cellular toxicity (7,11). As a result, targeting HER2^{positive} cancers with trastuzumab associates with a significant improved median OS compared to chemotherapy alone, including in GC (7).

However, the lack of target molecules in HER2^{negative} AGCs means that the first-line therapeutic options for these cancers remain limited to conventional chemotherapy (12). Consequently, there is strong demand for new therapeutic targets for HER2^{negative} AGCs.

It is now clear that tumor-infiltrating immune cells play critical roles in the development, progression, and metastasis of various cancers (13,14). These immune cells include T cells, which are currently the best characterized of these cells and have led to immunotherapies that largely aim to reinvigorate exhausted T cells and augment the anti-tumoral effects of these cells (15-18). These T cell-based immunotherapies promote OS in several cancer types. However, their clinical benefits remain limited in many patients due to the development of resistance to the immunotherapy (19-21). In relation to this, tumor-infiltrating myeloid cells have been shown recently to potently induce immunotherapy-resistant responses in cancer and to serve as master regulators of cancer progression (13,18,22-24). Thus, modulating these cells could have therapeutic effects, especially when combined with current T-cell immunotherapies. However, the myeloid cells in the TME remain poorly understood.

To address these issues, we used comprehensive multi-channel/multi-panel flow cytometric analysis to characterize the immune cells in the TME of 40 AGC samples, with particular focus on the myeloid cells in HER2^{negative} AGC. We show here that HER2^{negative} AGC associates with poor OS and enhanced neutrophil and non-classical monocyte infiltration that yields a high neutrophil-lymphocyte ratio. The putative pro-tumoral roles of neutrophils and non-classical monocytes in AGC are supported by an analysis of The Cancer Genome Atlas (TCGA) dataset, which showed that elevated expression of the signature genes for these 2 myeloid cell types in bulk gastrointestinal tumor specimens associated with poor OS. Moreover, these myeloid cells were present at higher frequencies in the HER2^{negative} AGCs of our patients. Thus, tumor neutrophils and non-classical monocytes may be potential therapeutic targets for HER2^{negative} AGC.

MATERIALS AND METHODS

Patients and specimens

GC tissues, adjacent normal stomach tissues, and blood samples were freshly obtained from patients with AGC who underwent surgical resection at Seoul National University Hospital. Patients with infectious diseases or autoimmune diseases were excluded. The HER2 molecular features of the AGCs were determined by histological examinations. T stage for each cancer was evaluated prior to surgery, and only patients with T2 or higher grade of cancer (AGC) were involved in this study. The study was approved by the Seoul National University Hospital Institutional Review Board (IRB approval No. 1905-087-1034) and was conducted in accordance with the tenets of the Declaration of Helsinki. Written informed consent was obtained from each subject. All patient data were anonymized.

Generation of single-cell suspensions from GC and adjacent normal tissues

The GC and normal tissues were chopped into small pieces and digested in RPMI-1640 (Biowest, L0498) containing 1 mg/ml collagenase type IV (LS004189; Worthington Biochemical Corp., Lakewood, NJ, USA), 1 mg/ml hyaluronidase (H6254; Sigma, Saint Louis, MO, USA), and 0.5 mg/ml DNase I (DN25; Sigma) for 30 min in a 37°C 5% CO_2 incubator. The digested tissues were then minced and filtered through a 70-μm cell strainer. The cells were pelleted by centrifugation and treated with 3 ml of 1x ACK lysis buffer (420301; Biolegend, San Diego, CA, USA) on ice for 5 min. The lysis reaction was stopped by adding 10 ml of 1× PBS. After centrifugation, the cell pellets were resuspended with 1 ml of RPMI supplemented with 10% FBS.

Generation of single-cell suspensions from patient blood

Blood was obtained by venipuncture and freshly collected in EDTA anticoagulant-coated Vacutainers (367525; BD Biosciences, San Jose, CA, USA). To remove the red blood cells, 3 ml of blood were transferred into a 50 ml tube that had been prefilled with 30 ml of 1x ACK lysis buffer (420301; Biolegend). After incubation on ice for 10 min, lysis was stopped by adding ice-cold 1x PBS. The leukocytes were pelleted by centrifugation and subjected to another round of ACK lysis. The pelleted cells were then resuspended with 1 ml of RPMI supplemented with 10% FBS.

Cell stimulation for cytokine profiling

To measure cytokine expression of CD8$^+$ T lymphocytes, the cells were stimulated with PMA (50 ng/ml) and Ionomycin (500 ng/ml) in 24 well plates for 4 h at 37°C, 5% CO_2. Brefeldin A

https://doi.org/10.4110/in.2021.21.e31

was also added for the accumulation of most cytokines at the Golgi complex/endoplasmic reticulum. After 4 hours incubation, the stimulation was stopped by adding the equal volume of RPMI supplemented with 10% FBS.

Flow cytometry

Single-cell suspensions from the GC tissues, adjacent normal tissues, and blood were washed with FACS-staining buffer (PBS with 0.5% BSA and 0.1% sodium azide) and then incubated with amine-reactive dead cell stain (L34961; Thermo Fisher Scientific, Waltham, MA, USA) for 30 min on ice. After another wash, the cells were stained with the following fluorescent-conjugated anti-human surface Abs for 20 min at 4°C: anti-human CD206 (19.2), anti-human CD11c (B-ly6), anti-human CD86 (IT2.2), anti-human CD15 (W6D3), anti-human CD68 (Y1/82A), anti-human CD66b (WM-53), anti-human CD14 (M5E2), anti-human CD16 (3G8), anti-human CD33 (G10F5), anti-human HLA-DR (L243), anti-human CD45 (HI30), anti-human CD11b (ICRF44), anti-human CD274 (MIH1), anti-human CXCR4 (12G5), anti-human CD56 (NCAM16.2), anti-human CD25 (2A3), anti-human CD19 (HIB19), anti-human CD8a (RPA-T8), anti-human CD4 (RPA-T4), anti-human Foxp3 (206D), anti-human NKP46 (9E2), anti-human PD-1 (EH12.2H7), anti-human IL-17A (BL-168), anti-human IFN-γ (4S. B3), anti-human TNF-α (Mab11), anti-human granzyme B (GB11). To stain intracellular Ags, the cells were first fixed and permeabilized with IC fixation buffer (00-8222-79; eBioscience, San Diego, CA, USA) and 1× permeabilization buffer (00-8333-56; eBioscience). The fixed and permeabilized cells were then stained with fluorescent-conjugated intracellular Abs for 1 hr at room temperature. For nuclear Foxp3 staining, the Foxp3 staining kit was used according to the manufacturer's instructions (00-5523-00; eBioscience). For intracellular cytokine staining, the cells were first stimulated in the presence of brefeldin A (420601; Biolegend) with 50 ng/ml PMA (P1585; Sigma) and 500 ng/ml ionomycin (I0634; Sigma) for 4 h in a 37°C 5% CO_2 incubator. All stained cells were washed and filtered through a 40-μm cell strainer and then analyzed on a LSRFortessa (BD Biosciences) or a FACSymphony A3 (BD Biosciences) flow cytometer.

Survival analysis and expression analysis

Kaplan-Meier OS analyses were performed with Gepia2 (25) for TCGA and Genotype-Tissue Expression incorporated datasets and Kaplan-Meier plotter (26,27) for TCGA and Gene Expression Omnibus (GEO; GSE22377) datasets. We have compared gene expressions among stomach adenocarcinoma, adjacent normal/healthy stomach and stomach cancer with Gepia2 (25).

Statistical analysis

All data are shown as mean ± SEM. Patients with $HER2^{positive}$/$HER2^{negative}$ AGCs or low/high expression of cell-specific molecular signatures were compared in terms of OS by generating Kaplan-Meier curves and comparing them with the logrank test. Hazard ratios (HRs) and 95% confidence intervals (CIs) for disease progression were also calculated. Patient groups were compared by unpaired or paired 2-tailed Student's *t*-test. The p-values of <0.05 were considered statistically significant ($p<0.05$, $p<0.01$, $p<0.001$). All statistical analyses were performed using GraphPad Prism (GraphPad Software, San Diego, CA, USA).

RESULTS

GC tissues, adjacent normal tissues, and blood were freshly obtained from 40 AGC patients undergoing surgery (**Fig. 1A**). The clinical and pathological characteristics of these patients are summarized in **Supplementary Table 1**. Thus, average patient age was 62.5±10 years, >82% were male, and 8 patients had received chemotherapy prior to surgery. The tumors were on average 6 cm in diameter and 53% were HER2^{negative}. Most patients had stage III (50%) or II (33%) disease, and MSS was the most common molecular subtype. Stage and microsatellite instability according to HER2 expression are briefly described by stacked bar plots in **Supplementary Fig. 1A**.

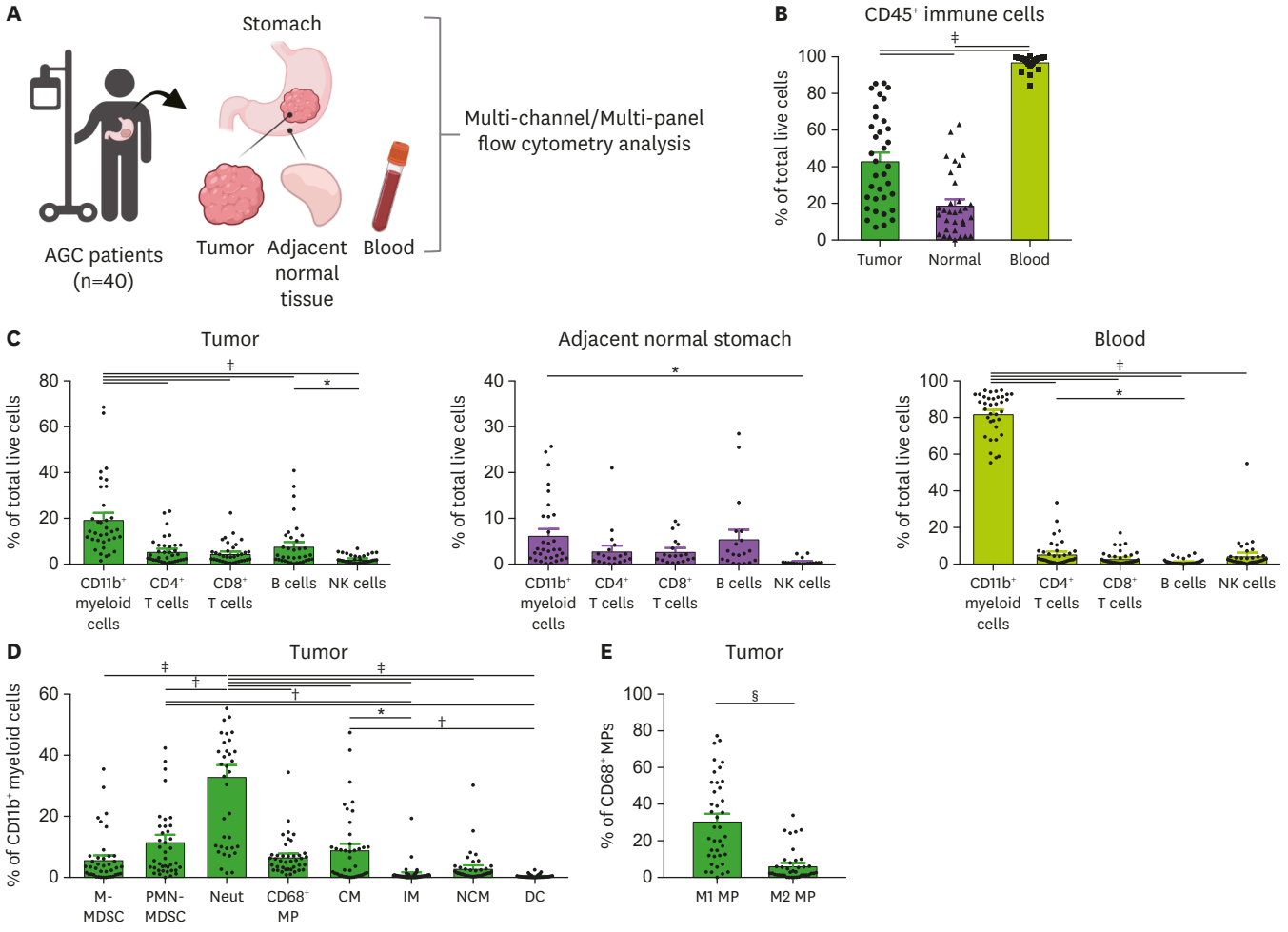

Figure 1. Depiction of human AGC immune profiling by multi-parametric flow cytometry and qualitative analysis of the immune profiles of the AGCs, adjacent normal stomach, and blood. (A) Tumor tissues, adjacent normal stomach tissues, and blood samples were freshly obtained from 40 patients with advanced gastric cancer who underwent surgical resection. The single-cell suspensions were stained as described in the materials and methods and then subjected to multi-channel/multi-panel flow cytometry. (B, C) Frequencies of CD45$^+$ immune cells (B) and the 5 main immune cell types (C) in the tumors, normal stomach, and blood relative to total live cell numbers, as determined by flow cytometry. (D) Frequencies of 8 major myeloid cell types relative to live CD11b$^+$ cell numbers in the gastric tumors. (E) Frequencies of M1- and M2-polarized macrophages in the gastric tumors relative to CD68$^+$ macrophage numbers. In (B-E), each symbol (dot, triangle, or square) indicates an individual sample (individual patient) and the data are shown as mean with SEM.
M-MDSC, monocytic myeloid-derived suppressor cells; Neut, neutrophils; MP, macrophages; CM, classical monocytes; IM, intermediate monocytes; NCM, non-classical monocytes; DC, dendritic cell.
$^*p<0.05$, $^\dagger p<0.01$, $^\ddagger p<0.001$ in the comparison across tissues and immune subsets, as determined by 1-way ANOVA; $^\S p<0.001$ in the comparison of M1-polarized macrophages and M2-polarized macrophages in tumor, as determined by 2-tailed Student's *t*-test.

https://doi.org/10.4110/in.2021.21.e31

Immune profiles of AGC tumors, normal stomach tissues, and blood, as determined by multi-channel/multi-panel flow cytometry

To comprehensively investigate the immune profiles, including the myeloid and lymphoid compartments, that associate with AGC, we established a multi-channel/multi-panel flow cytometry platform. Thus, single-cell suspensions from GC tissues, the adjacent normal tissues, and blood of the AGC patients first underwent gating with forward scatter area (FSC-A) and forward scatter height to remove the doublets. FSC-A and side scatter area gating was then conducted to remove the debris, after which the cells were incubated with amine-reactive dead cell stain to identify the live cells. The live cells were then stained for the pan-leukocyte marker CD45 and the $CD45^+$ cells were stained for the marker combinations indicated in **Supplementary Table 2**. **Supplementary Fig. 1B** depicts the gating strategy that was used to identify the various myeloid cell subsets.

Of the total live cells in the gastric TME, adjacent normal stomach, and blood, 43.4%, 19.2%, and 97.3% were $CD45^+$ immune cells, respectively (**Fig. 1B**). Thus, the adjacent normal stomach exhibited much less immune cell infiltration than the gastric TME. In all 3 tissues, $CD11b^+$ myeloid cells were the most frequent cell population (19.7%, 6.4%, and 82.6% of total live cells). Thus, the blood consisted largely of myeloid cells whereas the GCs and especially the normal stomach had fewer such cells. B cells were the next most common cell type in the GCs (8.0% of the total live cells); normal stomach and especially blood had fewer B cells (5.7% and 1.2%, respectively). $CD4^+$ T cells, the third most common cell type in GCs (5.8%), were less and equally common in the normal stomach and blood (3.0% and 5.8%, respectively). $CD8^+$ T cells tended to be slightly higher in the GCs than in the normal stomach and blood (4.8% *vs.* 2.9% and 3.3%, respectively). NK cells were the least common cell type in GCs (2.3%) and were even less common in the normal stomach (0.6%). However, the blood had higher frequencies of NK cells (4.8%) (**Fig. 1C**).

We next zoomed into the myeloid subsets in the gastric TME. Neutrophils accounted for the largest portion of tumor-infiltrating $CD11b^+$ myeloid cells (33.3%), followed by polymorphonuclear myeloid-derived suppressor cells (PMN-MDSCs) (11.9%), classical monocytes (9.2%), $CD68^+$ macrophages (6.9%), monocytic myeloid-derived suppressor cells (6.0%), and non-classical monocytes (3.1%). Intermediate monocytes and dendritic cells were rare (1.2% and 0.4%, respectively) (**Fig. 1D**). Since many previous studies suggest that classically activated M1 and alternatively activated M2 macrophages in the TME respectively associate with tumor-promoting and tumor-inhibiting activities (28), we also enumerated the M1 and M2 macrophages in the TME $CD68^+$ macrophage population (identified as $CD86^+$ $CD206^-$ and $CD86^-$ $CD206^+$ cells, respectively (28)). The gastric TME tended to associate with more M1 macrophage polarization (**Fig. 1E**). However, since recent studies have shown that the functional signatures of tumor-associated macrophages do not fit the M1/M2 model (29,30), the functional meaning of this phenotype in GC requires further analysis.

$HER2^{negative}$ AGCs associate with lower OS and significantly greater infiltration with neutrophils and non-classical monocytes

Next, we investigated the clinical impact of HER2 expression in terms of AGC progression. Kaplan-Meier OS curves with Asian GC TCGA dataset showed that low expression of HER2 associated significantly with poor patient prognosis (logrank p=0.048; HR [95% CIs], 0.31 [0.09–1.06]) (**Fig. 2A**).

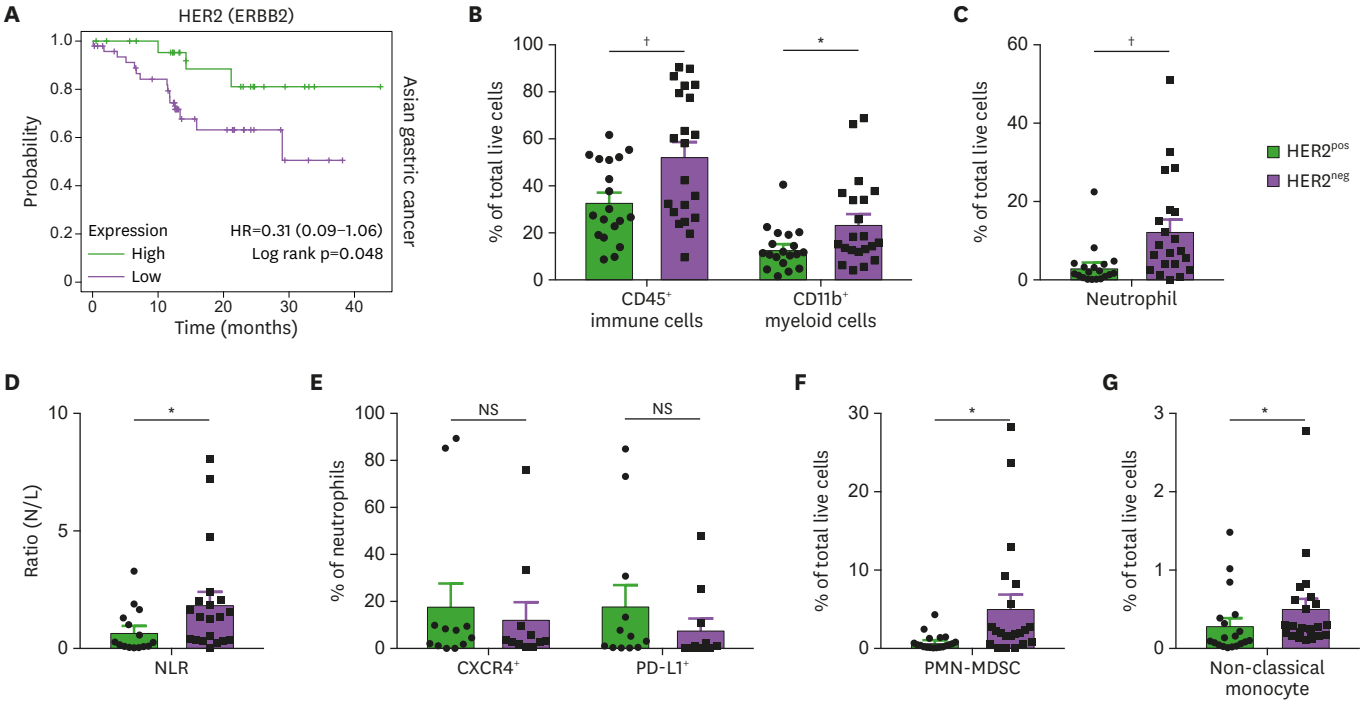

Figure 2. HER2^{negative} AGCs associate with lower OS and increased neutrophil and non-classical monocyte infiltration. (A) Kaplan-Meier OS curves of the Asian gastric cancer patients with low and high HER2 expression (TCGA dataset). (B-G) Flow cytometry analysis of the CD45$^+$ immune cells and CD11b$^+$ myeloid cells (B), neutrophils (C), NLR (D), CXCR4$^+$ and PD-L1$^+$ neutrophils (E), PMN-MDSCs (F), and non-classical monocytes (G) in the HER2^{pos} and HER2^{neg} gastric tumors. In (B-G), the circles and squares indicate individual HER2^{pos} and HER2^{neg} tumor specimens, respectively.
HER2^{pos}, HER2^{positive}; HER2^{neg}, HER2^{negative}; NLR, neutrophil-lymphocyte ratio; NS, not statistically significant.
*p<0.05, †p<0.01 in the comparison of HER2^{pos} and HER2^{neg} tumors, as determined by 2-tailed Student's *t*-tests.

To identify therapeutically targetable populations for HER2^{negative} AGC, we grouped the patients according to GC HER2 expression. In total, 19 and 21 of the patients had HER2^{positive} and HER2^{negative} AGCs, respectively. Flow cytometry analysis showed that compared to the HER2^{positive} GCs, the HER2^{negative} GCs were infiltrated with significantly more CD45$^+$ immune cells and CD11b$^+$ myeloid cells relative to total live cells (p=0.0099 and 0.0260 respectively; **Fig. 2B**).

A closer examination of the CD11b$^+$ myeloid cell compartment then showed that the HER2^{negative} tumors exhibited >3.8-fold greater infiltration of neutrophils compared to the HER2^{positive} tumors (p=0.0054; **Fig. 2C**). As a result, the HER2^{negative} tumors had higher neutrophil-to-lymphocyte ratios (p=0.0437; **Fig. 2D**). This is significant because high neutrophil-to-lymphocyte ratios associate with poor survival and are thus of prognostic value in many types of solid tumor (31,32). Since neutrophils are known to promote tumor immunotherapy resistance by expressing immunosuppressive molecules such as CXCR4 and PD-L1 (23,24), we also assessed the expression of these markers on the tumor neutrophils. However, we did not observe any significant differences between the 2 groups in terms of these markers (**Fig. 2E**).

In terms of other myeloid cell subsets, we also found that the HER2^{negative} tumors had significantly more PMN-MDSC than the HER2^{positive} tumors (p=0.0176; **Fig. 2F**). Moreover, the HER2^{negative} gastric tumors exhibited >1.7-fold greater infiltration of the TME with non-classical monocytes (p=0.0188; **Fig. 2G**). This is of interest because a recent study reported that in preclinical colon cancer, early infiltration of the TME with non-classical monocytes enhances the subsequent recruitment of neutrophils, which in turn promotes resistance responses to anti-angiogenic therapy and thereby accelerates disease progression (23,24).

Thus, high non-classical monocyte infiltration into the gastric TME may promote the greater neutrophil infiltration seen in HER2^{negative} gastric tumors.

These analyses show together that HER2^{negative} gastric tumors, which associate with poor OS, have higher frequencies of neutrophils, PMN-MDSCs, and non-classical monocytes. Notably, these immunological differences between HER2^{positive} and HER2^{negative} AGCs were not observed in the live cell populations from the normal adjacent stomach or blood of these patients (**Supplementary Fig. 2** and data not shown). Thus, tumor neutrophils, PMN-MDSCs, and non-classical monocytes potentially promote GC progression in HER2^{negative} AGC.

High expression of the molecular signatures of neutrophils and non-classical monocytes in gastrointestinal tumors in the TCGA database associates with poor OS

Here, we will focus further on the neutrophils and non-classical monocytes in the advanced gastric TME, since we will be reporting further studies on the PMN-MSDSCs in another paper. Thus, we next examined the immunogenomic sequences of 408 bulk stomach cancer and 211 normal stomach samples in the TCGA database to determine whether the molecular signatures of neutrophils and non-classical monocytes are more highly expressed in these cancer TMEs than in normal stomach samples. The neutrophil signature was defined with FCGR3A, CSF3R, S100A8, S100A9, MMP9, and CEACAM8, while CX3CR1, CXCR4, FCGR3B, and HLA-DRA served to define the non-classical monocyte signature. Indeed, the molecular signatures of both neutrophils and non-classical monocytes were expressed at significantly higher levels in the stomach cancer samples (**Supplementary Fig. 3A**). Of note, the mRNA expressions of chemokines that are involved in recruiting CXCR2^{+} neutrophils and CX3CR1^{+} non-classical monocytes were also significantly increased in the stomach cancer TMEs than in normal stomach (**Supplementary Fig. 3B**).

We then searched the immunogenomic sequences of the 1,508 bulk gastrointestinal cancer samples in TCGA dataset and the 43 bulk GC samples in GEO dataset for the neutrophil and non-classical monocyte signatures to determine whether high or low expression of these signatures associated with the OS of these patients. As a control, we also searched for the classical monocyte signature, which was defined as CD14, CCR2, CD36, SELL, and FCGR1B. Interestingly, Kaplan-Meier OS analysis showed that patients with low expression of the neutrophil and non-classical monocyte signatures had better OS (**Fig. 3A**, **Supplementary Fig. 3C**). By contrast, high or low classical monocyte signature expression did not associate with altered OS (**Fig. 3A**, **Supplementary Fig.3C**). Thus, high neutrophil and non-classical monocyte numbers in gastrointestinal tumors associate with worse OS. Notably, when we conducted the same analysis with all 9,396 solid cancers in the TCGA database, low and high expression of the neutrophil, non-classical monocyte, or classical monocyte signatures did not associate with different OS (**Fig. 3B**). This suggests that neutrophils and non-classical monocytes specifically promote poor outcomes in gastrointestinal tumors.

We next examined the association between neutrophil or non-classical monocyte frequencies in the TMEs of our 40 AGC patients and their cancer stage (stage I vs. stage II–IV). Advanced cancer stage associated with significantly greater neutrophil and non-classical monocyte infiltration (p=0.0469 and 0.0251, respectively; **Fig. 3C**). Since both cell types are more frequent in HER2^{negative} AGC than in HER2^{positive} AGC (**Fig. 2**), they could serve as potential therapeutic targets for this GC subtype.

https://doi.org/10.4110/in.2021.21.e31

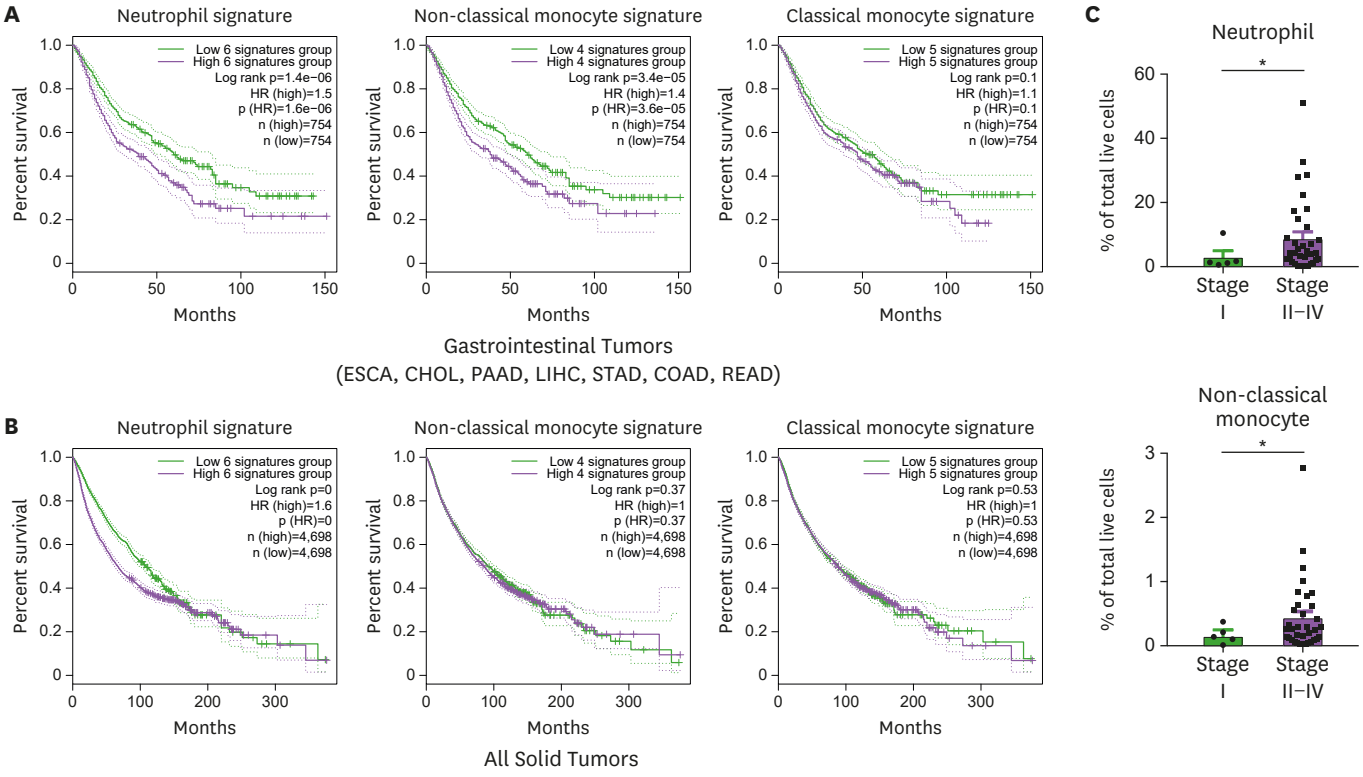

Figure 3. Patient survival analyses support the notion that neutrophils and non-classical monocytes have pro-tumoral features. (A, B) Patients with gastrointestinal tumors in the TCGA/Genotype-Tissue Expression database have better OS when they have low tumor expression of the molecular signatures of neutrophils and non-classical monocytes but not classical monocytes. In this analysis, patients with gastrointestinal tumors in the TCGA (defined by ESCA, CHOL, PAAD, LIHC, STAD, COAD, and READ expression) were grouped according to whether the expression of the molecular signatures of neutrophils (left), non-classical monocytes (middle), and classical monocytes (right) in the tumors was low or high. The neutrophil signature was defined by FCGR3A, CSF3R, S100A8, S100A9, MMP9, and CEACAM8. The non-classical monocyte signature was defined by CX3CR1, CXCR4, FCGR3B, and HLA-DRA. The classical monocyte signature was defined by CD14, CCR2, SELL, CD36, and FCGR1B. Kaplan-Meier OS curves of the high/low signature-expressing patients were generated and compared by logrank test. HR were also determined. (C) Flow cytometric analysis of the frequencies of neutrophils (above) and non-classical monocytes (below) in the stage I AGC and stage II–IV AGCs of our patient cohort.
*p<0.05 in the comparison of the 2 patient groups, as determined by 2-tailed Student's *t*-tests.

Increased neutrophil and non-classical monocyte infiltration in HER2^{negative} AGC does not associate with alterations in lymphoid population composition or function

Since our multi-channel/multi-panel flow cytometry platform allowed us to comprehensively and simultaneously analyze the entire immune cell composition in each sample, we were able to determine whether the greater infiltration of neutrophils and non-classical monocytes in HER2^{negative} AGC altered other immune features of these AGCs. However, the HER2^{negative} and HER2^{positive} AGCs did not differ significantly in terms of CD4$^+$ T cell, CD8$^+$ T cell, Fox3$^+$ Treg, B cell, or NK cell frequencies (**Fig. 4A**), the frequencies of CD8$^+$ T cells that expressed granzyme B, IFN-γ, IL-17A, or TNF-α (**Fig. 4B**), or the frequencies of CD4$^+$ T cells and CD8$^+$ T cells that expressed PD-1 (**Fig. 4C**). **Supplementary Fig. 4A and B** depict the gating strategy that was used to identify the various lymphoid subsets and their cytokine/PD-1 expressions. These observations together suggest that while neutrophils and non-classical monocytes may facilitate disease progression in HER2^{negative} AGC, their pro-tumoral functions may not be mediated by interactions with other lymphoid subsets.

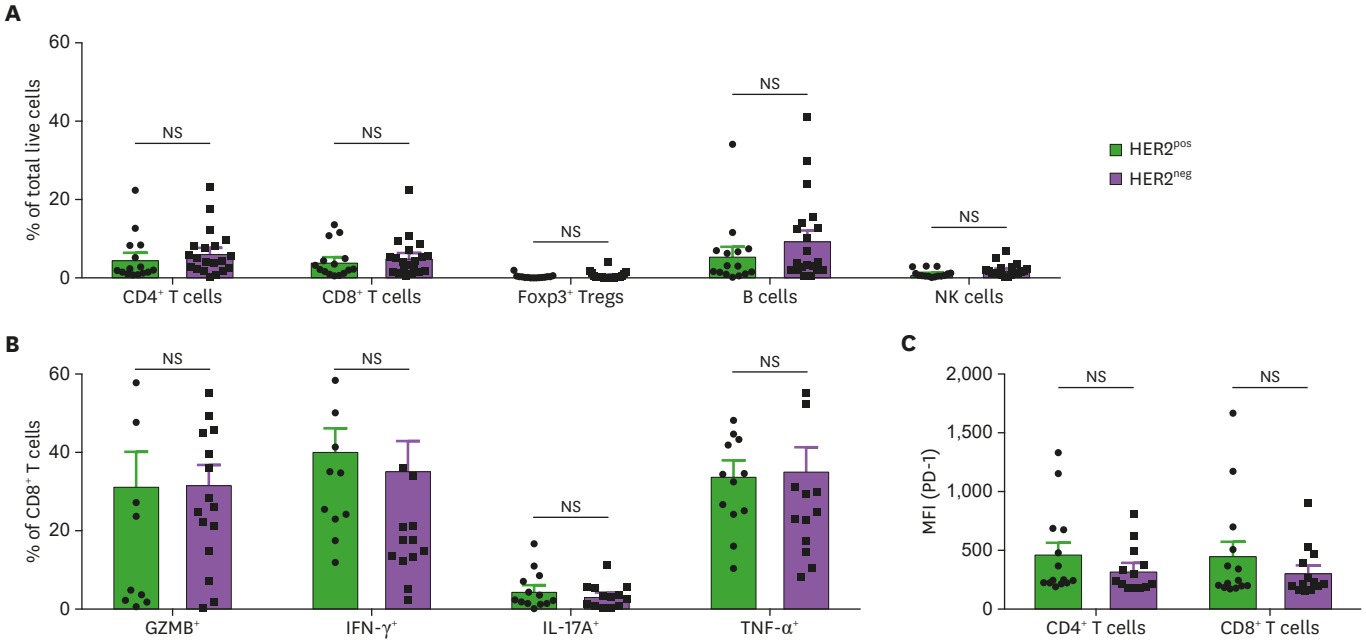

Figure 4. HER2^{pos} and HER2^{neg} AGC do not differ in terms of lymphoid subset frequencies or functions. (A-C) Flow cytometry comparison of the HER2^{pos} and HER2^{neg} gastric tumors in terms of the frequencies of lymphoid subsets (A), cytokine-expressing CD8$^+$ T cells (B), and MFI values of PD-1 expression on CD4$^+$ and CD8$^+$ T (C). Circles and squares indicate HER2^{pos} and HER2^{nega} AGC, respectively.
HER2^{pos}, HER2^{positive}; HER2^{neg}, HER2^{negative}; GZMB, granzyme B; NS, no significant difference, as measured by Student's *t*-test; MFI, mean fluorescence intensity.

DISCUSSION

Since HER2^{negative} AGC lack the targets of currently available cancer immunotherapies, patients with these tumors have few treatment options beyond chemotherapy. In the present study, we used a multi-panel/multi-channel flow cytometry platform to search for possible immunotherapy targets for HER2^{negative} AGC. We found that compared to HER2^{positive} AGCs, HER2^{negative} tumors both exhibited increased infiltration of neutrophils and non-classical monocytes and associated with worse OS. Moreover, high frequencies of neutrophils and non-classical monocytes in the TME associated with worse OS and AGC disease progression. These observations suggest that these myeloid subsets play a pro-tumoral role in HER2^{negative} AGC and thus may serve as novel therapeutic targets for these tumors.

Previous studies suggest that neutrophils in the TME can play both pro- and anti-tumoral roles depending on the type of cancer, the cancer stage, and the therapeutic regimen (13). With regard to human GC, it has been reported that enhanced infiltration of the TME with neutrophils associates with poor prognosis (33). This is supported by the findings in our study, namely, that greater neutrophil infiltration in the TME associated with advanced stage GC and worse OS.

With regard to non-classical monocytes, while several pre-clinical and clinical studies suggest that these cells have anti-tumoral properties (34-38), the preclinical studies of our group on colorectal cancer showed recently that non-classical monocytes may also play pro-tumoral roles. Specifically, they can recruit neutrophils to the TME and suppress local adaptive immunity by secreting IL-10; both of these activities induce resistance to anti-angiogenic therapy (23,24). Moreover, Sidibe et al. (39) recently reported with DLD_1 and HCT116 human colorectal cancer xenograft models that non-classical monocytes also promote angiogenesis,

thereby causing rapid cancer progression. This pro-tumoral role is supported by multiple studies showing that recruitment of Tie2-expressing monocytes (which may phenotypically belong to non-classical monocytes) to the vasculature in the TME switches on angiogenesis (40-43). Our present study also suggests that non-classical monocytes play pro-tumoral roles in AGC since higher frequencies of these cells associated with poor prognosis.

Immune checkpoint blockade, which promotes the anti-tumoral activities of T cells, is of clinical benefit for several cancers, including advanced stage melanoma, squamous and non-squamous non-small-cell lung carcinoma, and kidney carcinoma (44-46). However, this therapy performs below expectations in AGC. Specifically, although the United States Food and Drug Administration has approved pembrolizumab, a humanized monoclonal Ab that inhibits PD-1, for some patients with AGC, it does not significantly improve OS or progression-free survival in patients with PD-L1^{positive} AGC (7). This limited clinical benefit of current T cell-based immunotherapies reflects our poor understanding of the complicated cellular interactions that take place in the TME and can mediate therapy resistance. To increase the efficacy of immunotherapies in more patients, it will be necessary to elucidate the heterogeneity of tumor-infiltrating cells and delineate the functional roles that they play in the TME. Of particular interest are the myeloid cells because they have been suggested to be master regulators of drug resistance in cancer (13,23,24).

The present study has several limitations. First, how neutrophils and non-classical monocytes may promote GC progression and poor OS remains unclear. However, our analyses in **Fig. 4** suggest that these pro-tumoral roles do not reflect an impact of these cells on the frequencies of T, B, and NK cells, or T cell subsets or functions, in the TME. In future studies, we aim to elucidate the pro-tumoral mechanisms of neutrophils and non-classical monocytes in AGC by establishing pre-clinical *in vivo* models of HER2^{negative} and HER2^{positive} GC and then comparing them in terms of their immune compartment in the TME. Although our flow cytometry immune profiles and bulk-seq data of human GC specimens characterized HER2^{negative} AGC with an increase of neutrophils and non-classical monocytes, it is still unclear whether the increase of neutrophils and non-classical monocytes in GC is the cause or result of advanced stage. Therefore, we plan to address these questions through follow-up studies including Ab-mediated *in vivo* depletion of neutrophils and/or non-classical monocytes in pre-clinical models of HER2^{negative} GCs. Furthermore, we will investigate how neutrophils and non-classical monocytes interact with other cells in the TME and how these interactions and other activities regulate tumor progression. The second limitation of the present study relates to our multi-parametric flow cytometry analysis: while it allowed us to analyze multiple cell types in the same specimen, its ability to comprehensively analyze phenotypically/functionally heterogenous cell types was limited due to the still-partial knowledge regarding cell type-specific signatures. This issue could be improved by using more unbiased methods such as single-cell RNA sequencing. This high-dimensional technology has been shown recently to both delineate the cellular heterogeneity in various cancers and unveil the complicated regulatory interactions of multiple genes in unprecedented detail. This approach has led recently to novel insights and new therapeutic targets for multiple cancers (29,30,35,47-55).

In summary, we showed that high TME frequencies of neutrophils and non-classical monocytes associated with AGC progression and poor OS. Moreover, both of these 2 pro-tumoral myeloid subsets were more frequent in the TME of HER2^{negative} AGC compared to HER2^{positive} AGC. This strongly suggests that neutrophils and non-classical monocytes may be potential therapeutic targets for HER2^{negative} AGC.

ACKNOWLEDGEMENTS

This work was supported by the National Research Foundation of Korea (NRF) grant funded by the Korea government (MSIT) (No. 2020R1C1C1015062) (K.J.), by the cooperative Research Program of Basic Medical Science and Clinical Science from the Seoul National University College of Medicine (No. 800-20190261) (K.J.)/(No. 800-20190262) (H.K.Y.), by the SNUH Research Fund 03-2018-0290 (K.J.), by the Creative-Pioneering Researchers Program through Seoul National University (SNU) (K.J.), and by the Basic Research Program through the National Research Foundation of Korea (NRF) funded by the MSIT (NRF-2020R1A4A1017515) (K.J.).

SUPPLEMENTARY MATERIALS

Supplementary Table 1
Clinical characteristics of AGC patients

Click here to view

Supplementary Table 2
Markers for flow cytometric analysis of immune cell populations

Click here to view

Supplementary Figure 1
(A) Stacked bar plots that compare ages (left), overall stages (middle), and microsatellites (right) between $HER2^{pos}$ and $HER2^{neg}$ gastric cancer patient specimens in this study. (B) The cell gating strategy used in our multi-channel/multi-panel flow cytometry platform to identify the multiple human myeloid cell subsets in each sample. Representative plots are shown.

Click here to view

Supplementary Figure 2
Comparison of the frequencies of neutrophils and non-classical monocytes in the blood (A) and adjacent normal stomach (B) samples from the patients with $HER2^{pos}$ and $HER2^{neg}$ AGC.

Click here to view

Supplementary Figure 3
(A) Box plots showing the expression level of the neutrophil (left) and non-classical monocyte (right) molecular signatures in the 408 stomach adenocarcinoma and 211 normal stomach samples in the TCGA/GTEx database. (B) Box plots showing the expression level of CXCL1, CXCL2, CXCL3, CXCL5, and CX3CL1 in 408 stomach adenocarcinoma and 211 normal stomach samples in the TCGA/GTEx database. (C) Patients with gastric cancer in GEO dataset were grouped according to whether the expression of the molecular signatures of neutrophils (left), non-classical monocytes (middle), and classical monocytes (right) in the tumors was low or high. The neutrophil signature was defined by FCGR3A, CSF3R, S100A8, S100A9, MMP9, and CEACAM8. The non-classical monocyte signature was defined by CX3CR1, CXCR4, FCGR3B, and HLA-DRA. The classical monocyte signature was defined by

CD14, CCR2, SELL, CD36, and FCGR1B. Kaplan-Meier OS curves of the high/low signature-expressing patients were generated and compared by logrank test. HR were also determined.

Click here to view

Supplementary Figure 4

(A) The cell gating strategy used in our multi-channel/multi-panel flow cytometry platform to identify the human lymphoid cell subsets ($CD8^+$ T cells, $CD4^+$ T cells, B cells, and NK cells) in each sample. Representative plots are shown. (B) For cytokine panel, cells were stained after 4 h stimulation with PMA/ionomycin. Representative plots of gating strategy for the indicated cytokine expressions are shown. Molecular characteristics after stimulation were featured with decreased levels of CD3 and CD4 expressions.

Click here to view

REFERENCES

1. Etemadi A, Safiri S, Sepanlou SG, Ikuta K, Bisignano C, Shakeri R, Amani M, Fitzmaurice C, Nixon M, Abbasi N, et al. The global, regional, and national burden of stomach cancer in 195 countries, 1990–2017: a systematic analysis for the Global Burden of Disease study 2017. *Lancet Gastroenterol Hepatol* 2020;5:42-54.
PUBMED | CROSSREF
2. Sung H, Ferlay J, Siegel RL, Laversanne M, Soerjomataram I, Jemal A, Bray F. Global cancer statistics 2020: GLOBOCAN estimates of incidence and mortality worldwide for 36 cancers in 185 countries. *CA Cancer J Clin* 2021;71:209-249.
PUBMED | CROSSREF
3. Kono K, Nakajima S, Mimura K. Current status of immune checkpoint inhibitors for gastric cancer. *Gastric Cancer* 2020;23:565-578.
PUBMED | CROSSREF
4. Shi WJ, Gao JB. Molecular mechanisms of chemoresistance in gastric cancer. *World J Gastrointest Oncol* 2016;8:673-681.
PUBMED | CROSSREF
5. Masuishi T, Kadowaki S, Kondo M, Komori A, Sugiyama K, Mitani S, Honda K, Narita Y, Taniguchi H, Ura T, et al. FOLFOX as first-line therapy for gastric cancer with severe peritoneal metastasis. *Anticancer Res* 2017;37:7037-7042.
PUBMED | CROSSREF
6. Madden EC, Gorman AM, Logue SE, Samali A. Tumour cell secretome in chemoresistance and tumour recurrence. *Trends Cancer* 2020;6:489-505.
PUBMED | CROSSREF
7. Joshi SS, Badgwell BD. Current treatment and recent progress in gastric cancer. *CA Cancer J Clin* 2021;71:264-279.
PUBMED | CROSSREF
8. Tsapralis D, Panayiotides I, Peros G, Liakakos T, Karamitopoulou E. Human epidermal growth factor receptor-2 gene amplification in gastric cancer using tissue microarray technology. *World J Gastroenterol* 2012;18:150-155.
PUBMED | CROSSREF
9. Shitara K, Bang YJ, Iwasa S, Sugimoto N, Ryu MH, Sakai D, Chung HC, Kawakami H, Yabusaki H, Lee J, et al. Trastuzumab deruxtecan in previously treated HER2-positive gastric cancer. *N Engl J Med* 2020;382:2419-2430.
PUBMED | CROSSREF
10. Yang YM, Hong P, Xu WW, He QY, Li B. Advances in targeted therapy for esophageal cancer. *Signal Transduct Target Ther* 2020;5:229.
PUBMED | CROSSREF
11. Vu T, Claret FX. Trastuzumab: updated mechanisms of action and resistance in breast cancer. *Front Oncol* 2012;2:62.
PUBMED | CROSSREF

12. Yao Y, Deng R, Liao D, Xie H, Zuo J, Jia Y, Kong F. Maintenance treatment in advanced HER2-negative gastric cancer. *Clin Transl Oncol* 2020;22:2206-2212.
PUBMED | CROSSREF
13. Jeong J, Suh Y, Jung K. Context drives diversification of monocytes and neutrophils in orchestrating the tumor microenvironment. *Front Immunol* 2019;10:1817.
PUBMED | CROSSREF
14. Barnes TA, Amir E. HYPE or HOPE: the prognostic value of infiltrating immune cells in cancer. *Br J Cancer* 2017;117:451-460.
PUBMED | CROSSREF
15. Waldman AD, Fritz JM, Lenardo MJ. A guide to cancer immunotherapy: from T cell basic science to clinical practice. *Nat Rev Immunol* 2020;20:651-668.
PUBMED | CROSSREF
16. Jeong S, Park SH. Co-stimulatory receptors in cancers and their implications for cancer immunotherapy. *Immune Netw* 2020;20:e3.
PUBMED | CROSSREF
17. Kwon M, Choi YJ, Sa M, Park SH, Shin EC. Two-round mixed lymphocyte reaction for evaluation of the functional activities of anti-PD-1 and immunomodulators. *Immune Netw* 2018;18:e45.
PUBMED | CROSSREF
18. Kuen DS, Kim BS, Chung Y. IL-17-producing cells in tumor immunity: friends or foes? *Immune Netw* 2020;20:e6.
PUBMED | CROSSREF
19. Bonaventura P, Shekarian T, Alcazer V, Valladeau-Guilemond J, Valsesia-Wittmann S, Amigorena S, Caux C, Depil S. Cold tumors: a therapeutic challenge for immunotherapy. *Front Immunol* 2019;10:168.
PUBMED | CROSSREF
20. Restifo NP, Smyth MJ, Snyder A. Acquired resistance to immunotherapy and future challenges. *Nat Rev Cancer* 2016;16:121-126.
PUBMED | CROSSREF
21. Oh SJ, Lee J, Kim Y, Song KH, Cho E, Kim M, Jung H, Kim TW. Far beyond cancer immunotherapy: reversion of multi-malignant phenotypes of immunotherapeutic-resistant cancer by targeting the NANOG signaling axis. *Immune Netw* 2020;20:e7.
PUBMED | CROSSREF
22. Sharma P, Hu-Lieskovan S, Wargo JA, Ribas A. Primary, adaptive, and acquired resistance to cancer immunotherapy. *Cell* 2017;168:707-723.
PUBMED | CROSSREF
23. Jung K, Heishi T, Incio J, Huang Y, Beech EY, Pinter M, Ho WW, Kawaguchi K, Rahbari NN, Chung E, et al. Targeting CXCR4-dependent immunosuppressive Ly6C^{low} monocytes improves antiangiogenic therapy in colorectal cancer. *Proc Natl Acad Sci U S A* 2017;114:10455-10460.
PUBMED | CROSSREF
24. Jung K, Heishi T, Khan OF, Kowalski PS, Incio J, Rahbari NN, Chung E, Clark JW, Willett CG, Luster AD, et al. Ly6Clo monocytes drive immunosuppression and confer resistance to anti-VEGFR2 cancer therapy. *J Clin Invest* 2017;127:3039-3051.
PUBMED | CROSSREF
25. Tang Z, Kang B, Li C, Chen T, Zhang Z. GEPIA2: an enhanced web server for large-scale expression profiling and interactive analysis. *Nucleic Acids Res* 2019;47:W556-W560.
PUBMED | CROSSREF
26. Szász AM, Lánczky A, Nagy Á, Förster S, Hark K, Green JE, Boussioutas A, Busuttil R, Szabó A, Győrffy B. Cross-validation of survival associated biomarkers in gastric cancer using transcriptomic data of 1,065 patients. *Oncotarget* 2016;7:49322-49333.
PUBMED | CROSSREF
27. Nagy Á, Munkácsy G, Győrffy B. Pancancer survival analysis of cancer hallmark genes. *Sci Rep* 2021;11:6047.
PUBMED | CROSSREF
28. Bertani FR, Mozetic P, Fioramonti M, Iuliani M, Ribelli G, Pantano F, Santini D, Tonini G, Trombetta M, Businaro L, et al. Classification of M1/M2-polarized human macrophages by label-free hyperspectral reflectance confocal microscopy and multivariate analysis. *Sci Rep* 2017;7:8965.
PUBMED | CROSSREF
29. Azizi E, Carr AJ, Plitas G, Cornish AE, Konopacki C, Prabhakaran S, Nainys J, Wu K, Kiseliovas V, Setty M, et al. Single-cell map of diverse immune phenotypes in the breast tumor microenvironment. *Cell* 2018;174:1293-1308.e36.
PUBMED | CROSSREF

30. Zhang L, Li Z, Skrzypczynska KM, Fang Q, Zhang W, O'Brien SA, He Y, Wang L, Zhang Q, Kim A, et al. Single-cell analyses inform mechanisms of myeloid-targeted therapies in colon cancer. *Cell* 2020;181:442-459.e29.
PUBMED | CROSSREF

31. Shibutani M, Maeda K, Nagahara H, Noda E, Ohtani H, Nishiguchi Y, Hirakawa K. A high preoperative neutrophil-to-lymphocyte ratio is associated with poor survival in patients with colorectal cancer. *Anticancer Res* 2013;33:3291-3294.
PUBMED

32. Howard R, Kanetsky PA, Egan KM. Exploring the prognostic value of the neutrophil-to-lymphocyte ratio in cancer. *Sci Rep* 2019;9:19673.
PUBMED | CROSSREF

33. Zhao JJ, Pan K, Wang W, Chen JG, Wu YH, Lv L, Li JJ, Chen YB, Wang DD, Pan QZ, et al. The prognostic value of tumor-infiltrating neutrophils in gastric adenocarcinoma after resection. *PLoS One* 2012;7:e33655.
PUBMED | CROSSREF

34. Plebanek MP, Angeloni NL, Vinokour E, Li J, Henkin A, Martinez-Marin D, Filleur S, Bhowmick R, Henkin J, Miller SD, et al. Pre-metastatic cancer exosomes induce immune surveillance by patrolling monocytes at the metastatic niche. *Nat Commun* 2017;8:1319.
PUBMED | CROSSREF

35. Lavin Y, Kobayashi S, Leader A, Amir ED, Elefant N, Bigenwald C, Remark R, Sweeney R, Becker CD, Levine JH, et al. Innate immune landscape in early lung adenocarcinoma by paired single-cell analyses. *Cell* 2017;169:750-765.e17.
PUBMED | CROSSREF

36. Kubo H, Mensurado S, Gonçalves-Sousa N, Serre K, Silva-Santos B. Primary tumors limit metastasis formation through induction of IL15-mediated cross-talk between patrolling monocytes and NK cells. *Cancer Immunol Res* 2017;5:812-820.
PUBMED | CROSSREF

37. Romano E, Kusio-Kobialka M, Foukas PG, Baumgaertner P, Meyer C, Ballabeni P, Michielin O, Weide B, Romero P, Speiser DE. Ipilimumab-dependent cell-mediated cytotoxicity of regulatory T cells *ex vivo* by nonclassical monocytes in melanoma patients. *Proc Natl Acad Sci U S A* 2015;112:6140-6145.
PUBMED | CROSSREF

38. Hanna RN, Cekic C, Sag D, Tacke R, Thomas GD, Nowyhed H, Herrley E, Rasquinha N, McArdle S, Wu R, et al. Patrolling monocytes control tumor metastasis to the lung. *Science* 2015;350:985-990.
PUBMED | CROSSREF

39. Sidibe A, Ropraz P, Jemelin S, Emre Y, Poittevin M, Pocard M, Bradfield PF, Imhof BA. Angiogenic factor-driven inflammation promotes extravasation of human proangiogenic monocytes to tumours. *Nat Commun* 2018;9:355.
PUBMED | CROSSREF

40. Coffelt SB, Tal AO, Scholz A, De Palma M, Patel S, Urbich C, Biswas SK, Murdoch C, Plate KH, Reiss Y, et al. Angiopoietin-2 regulates gene expression in TIE2-expressing monocytes and augments their inherent proangiogenic functions. *Cancer Res* 2010;70:5270-5280.
PUBMED | CROSSREF

41. De Palma M, Murdoch C, Venneri MA, Naldini L, Lewis CE. Tie2-expressing monocytes: regulation of tumor angiogenesis and therapeutic implications. *Trends Immunol* 2007;28:519-524.
PUBMED | CROSSREF

42. De Palma M, Venneri MA, Roca C, Naldini L. Targeting exogenous genes to tumor angiogenesis by transplantation of genetically modified hematopoietic stem cells. *Nat Med* 2003;9:789-795.
PUBMED | CROSSREF

43. Murdoch C, Tazzyman S, Webster S, Lewis CE. Expression of Tie-2 by human monocytes and their responses to angiopoietin-2. *J Immunol* 2007;178:7405-7411.
PUBMED | CROSSREF

44. Decatris MP, O'Byrne KJ. Immune checkpoint inhibitors as first-line and salvage therapy for advanced non-small-cell lung cancer. *Future Oncol* 2016;12:1805-1822.
PUBMED | CROSSREF

45. Bai R, Lv Z, Xu D, Cui J. Predictive biomarkers for cancer immunotherapy with immune checkpoint inhibitors. *Biomark Res* 2020;8:34.
PUBMED | CROSSREF

46. Murciano-Goroff YR, Warner AB, Wolchok JD. The future of cancer immunotherapy: microenvironment-targeting combinations. *Cell Res* 2020;30:507-519.
PUBMED | CROSSREF

47. Venteicher AS, Tirosh I, Hebert C, Yizhak K, Neftel C, Filbin MG, Hovestadt V, Escalante LE, Shaw ML, Rodman C, et al. Decoupling genetics, lineages, and microenvironment in IDH-mutant gliomas by single-cell RNA-seq. *Science* 2017;355:eaai8478.
PUBMED | CROSSREF

48. Chevrier S, Levine JH, Zanotelli VRT, Silina K, Schulz D, Bacac M, Ries CH, Ailles L, Jewett MAS, Moch H, et al. An immune atlas of clear cell renal cell carcinoma. *Cell* 2017;169:736-749.e18.
PUBMED | CROSSREF

49. Gubin MM, Esaulova E, Ward JP, Malkova ON, Runci D, Wong P, Noguchi T, Arthur CD, Meng W, Alspach E, et al. High-dimensional analysis delineates myeloid and lymphoid compartment remodeling during successful immune-checkpoint cancer therapy. *Cell* 2018;175:1014-1030.e19.
PUBMED | CROSSREF

50. Zhang Q, He Y, Luo N, Patel SJ, Han Y, Gao R, Modak M, Carotta S, Haslinger C, Kind D, et al. Landscape and dynamics of single immune cells in hepatocellular carcinoma. *Cell* 2019;179:829-845.e20.
PUBMED | CROSSREF

51. Binnewies M, Mujal AM, Pollack JL, Combes AJ, Hardison EA, Barry KC, Tsui J, Ruhland MK, Kersten K, Abushawish MA, et al. Unleashing type-2 dendritic cells to drive protective antitumor $CD4^+$ T cell immunity. *Cell* 2019;177:556-571.e16.
PUBMED | CROSSREF

52. Zilionis R, Engblom C, Pfirschke C, Savova V, Zemmour D, Saatcioglu HD, Krishnan I, Maroni G, Meyerovitz CV, Kerwin CM, et al. Single-cell transcriptomics of human and mouse lung cancers reveals conserved myeloid populations across individuals and species. *Immunity* 2019;50:1317-1334.e10.
PUBMED | CROSSREF

53. Sathe A, Grimes SM, Lau BT, Chen J, Suarez C, Huang RJ, Poultsides G, Ji HP. Single-cell genomic characterization reveals the cellular reprogramming of the gastric tumor microenvironment. *Clin Cancer Res* 2020;26:2640-2653.
PUBMED | CROSSREF

54. Kim N, Kim HK, Lee K, Hong Y, Cho JH, Choi JW, Lee JI, Suh YL, Ku BM, Eum HH, et al. Single-cell RNA sequencing demonstrates the molecular and cellular reprogramming of metastatic lung adenocarcinoma. *Nat Commun* 2020;11:2285.
PUBMED | CROSSREF

55. Alshetaiwi H, Pervolarakis N, McIntyre LL, Ma D, Nguyen Q, Rath JA, Nee K, Hernandez G, Evans K, Torosian L, et al. Defining the emergence of myeloid-derived suppressor cells in breast cancer using single-cell transcriptomics. *Sci Immunol* 2020;5:eaay6017.
PUBMED | CROSSREF